Front. Electr. Electron. Eng. China 2007, 2(1): 78–82
DOI 10.1007/s11460-007-0014-y

RESEARCH ARTICLE

WAN Zhujun, WU Yaming, LI Sihua

Experimental research on an integrated thermooptic switch based on multimode interference couplers

Abstract The experimental results of a 2×2 integrated thermooptic Mach-Zehnder interferometer (MZI) switch based on multimode interference (MMI) couplers are reported. The insertion loss (IL) is 3.40 dB, the polarization dependent loss is 0.47 dB, the extinction ratio (ER) at bar state and cross state is 32.01 dB and 16.42 dB respectively, the response time is less than 3 ms, and the power consumption is 658 mW. Regarding the asymmetry of extinction ratio at bar state and cross state, theoretical analysis is first presented. The coupling ratio of the two MMI couplers deviates from 50 : 50 but the deviation is nearly the same, which is decided by good uniformity of semiconductor planar lightwave circuit (PLC) process. This property affects the extinction ratio at bar state and cross state in different mechanisms. Adding a metal electrode on the waveguide affects its effective index and analysis based on experimental results is given. The increment of waveguide effective index is in the order of 2×10^{-4}.

Keywords integrated optics, thermooptic switch, MMI coupler, MZI

1 Introduction

Optical switch is one of the key devices in intelligent optical network. It shows variable styles and can be classified as waveguide-based and free-space optical switch according to signal transfer method. Mechanical optical switch is a typical realization of free-space optical switch, including traditional mechanical optical switch and micro-electro-mechanical-systems (MEMS) optical switch. Traditional mechanical optical switch has been put into commercial applications such as line protection and monitoring, network reconfiguration and test equipments due to its technical maturity and good reliability. Two-dimensional MEMS optical switch is also commercially applied in line exchange due to its technical maturity and large scale [1,2] capabilities. Waveguide-based optical switch attracts the interests of researchers, which is characterized by its small size and convenience in integration It also shows variable styles, such as electro-optical switch based on $LiNbO_3$ waveguide, digital thermooptic switch based on Y-branch, bifurcation optically active (BOA) thermooptic switch based on a directional coupler, thermooptic Mach-Zehnder interferometer (MZI) switch based on the directional coupler and MZI thermooptic switch based on multimode interference (MMI), etc. [3–9].

Compared with directional couplers, MMI couplers show better uniformity and bandwidth and are more suitable for MZI type optical switch. In Ref. [9], a 2×2 thermooptic switch based on MMI couplers and Si/SiO_2 material is reported. Its IL is 1 dB, extinction ratio (ER) is 21 dB, response time is 180 μs and power consumption is 110 mW. Ref. [3] reports a 2×2 thermooptic switch based on MMI couplers and silicon on insulator (SOI) material. Its ER is 17.1 dB and power consumption is 235 mW. Here we report experimental results of a 2×2 thermooptic switch based on MMI couplers and Si/SiO_2 material. We observed asymmetrical ER between bar state and cross state and presented theoretical analysis for the first time. These experimental results are the basis for further optimization.

Translated from *Acta Optica Sinica*, 2006, 26(8): 1187–1191 [译自: 光学学报]

WAN Zhujun (✉), WU Yaming, LI Sihua
State Key Laboratory of Transducer Technology, Shanghai Institute of Microsystem and Information Technology, Chinese Academy of Sciences, Shanghai 200050, China
E-mail: wanzhujun@mail.sim.ac.cn

WAN Zhujun
Graduate School of the Chinese Academy of Sciences, Beijing 100049, China

2 Principles and parameters

Structure of the waveguide-based thermooptic switch is shown in Fig. 1, which is composed of two 3 dB 2×2 MMI couplers and a MZI. Heating electrode is added on one of the MZI arms. Phase relation of the MZI arms is controlled by thermooptic effect and connection of the switch is transferred between bar state (bar: port 1→1′ & 2→2′) and cross state (cross: port 1→2′ & 2→1′).

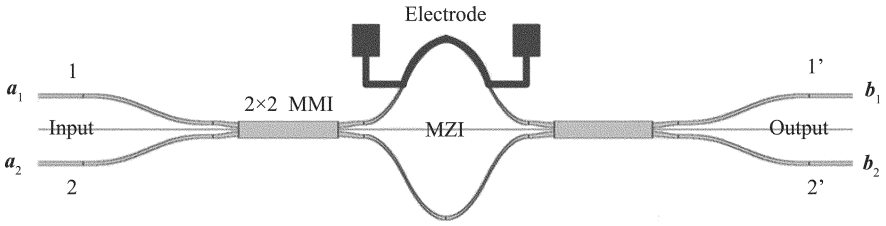

Fig. 1 Structure of the MMI based 2 × 2 optical switch

Multimode waveguide shows self-imaging property. Light splitting can be realized by setting access waveguides on imaging positions for special multimode waveguide length [10,11]. The parameters are designed according to the method described in Ref. [11] and are simulated with beam propagation method (BPM) software by Optiwave Inc. Simulation results of the 3 dB 2 × 2 MMI are splitting ratio = 49.74% : 50.26% and excess loss (EL) = 0.20 dB. The two MZI arms are separated through arc waveguides to reduce optical and thermal coupling there between. The electrode material is Ta_2N, which is more thermally resistant and conglutinative to the SiO_2 surface. The lead material is Cu and the resistance of the electrode is about 600 Ω.

Transfer matrix of the optical switch is shown in Eq. (1). The connection is cross state when $\phi = 2m\pi$ and bar state when $\phi = 2m\pi + \pi$.

$$\boldsymbol{T}_{\mathrm{sw}} = \begin{vmatrix} \sin\dfrac{\phi}{2} & -\cos\dfrac{\phi}{2} \\ -\cos\dfrac{\phi}{2} & -\sin\dfrac{\phi}{2} \end{vmatrix} \tag{1}$$

In order to switch the connection state, phase difference of the MZI arms needs to be changed by π, i.e. the optical path difference needs to be changed by $\lambda_0/2$. With thermooptic coefficient of SiO_2 $\mathrm{d}n/\mathrm{d}T = 1 \times 10^{-5}/°\mathrm{C}$, length of the electrode $L_e = 3$ mm, central wavelength $\lambda_0 = 1.55$ μm, temperature of the waveguide core needs to be changed by $\Delta T = 26$ K according to Eq. (2).

$$L_e \Delta T \frac{\mathrm{d}n}{\mathrm{d}T} = \frac{\lambda_0}{2} \tag{2}$$

3 Fabrication and test

3.1 Fabrication process

Embedded Si/SiO_2 waveguide was used and the waveguide section is shown in Fig. 2(b). Material of the waveguide core is Ge-doped SiO_2 and the section size is 5.5 μm × 5.5 μm. The lower and upper cladding is SiO_2 with a thickness of 15 μm. The core/cladding refractive index (RI) is 1.455/1.444 and the RI difference is 0.75%.

Fabrication process of the switch chip is shown in Fig. 2. The first step is to fabricate Si/SiO_2 waveguide on a Si substrate through chemical vapor deposition (CVD) and reactive ion etching (RIE) process, the sectional view is shown in Fig. 2(b). The second step is to scatter Ta_2N of 2 000 Å thickness and Cu of 1 μm thickness on the chip, the sectional view is shown in Fig. 2(c). The third step is to define electrode lead and welding pad of Cu material through wet etching, and Fig. 2(d) is the top view. The forth step is to define the electrode through the RIE process, and Fig. 2(e) is

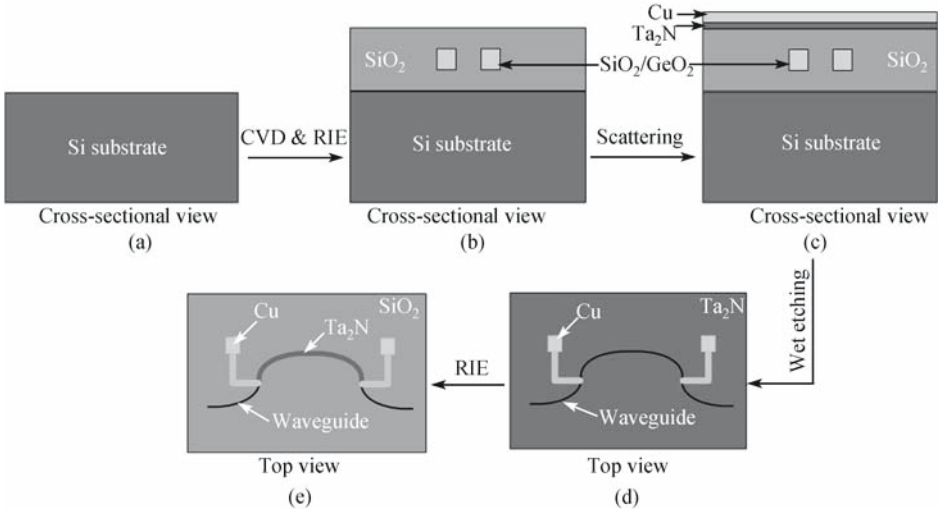

Fig. 2 Fabrication process of the switch chip

the top view showing the electrode, lead and pad of the finished chip. Finally, the chip endfaces were polished and the chip was set on a printed circuit board (PCB). The first step was finished in ANDevices Inc. and the other steps were finished in our institute. The device size is 23.5 mm × 0.4 mm including access waveguides on both ends.

3.2 Relationship between output and driving power

The test equipments include tunable laser (output wavelength is set to 1.55 μm) module of EXFO IQS12004B DWDM optical passive devices test system and Advantest Q8221 multi-channel power meter. The access waveguides are coupled with two fiber arrays (FA) and adjusted with Suruga six-dimensional auto-adjusting system. The relationship between the driving power (measured resistance of electrode is 515 Ω and thus driving voltage is converted into driving power) and loss of each output was measured and shown in Fig. 3, where Fig. 3(a) corresponds to input from port 1 and Fig. 3(b) corresponds to input from port 2. The bottom positions of each curve correspond to necessary driving power to keep bar state or cross state. Corresponding IL, crosstalk and ER are listed in Table 1, including coupling loss with FAs.

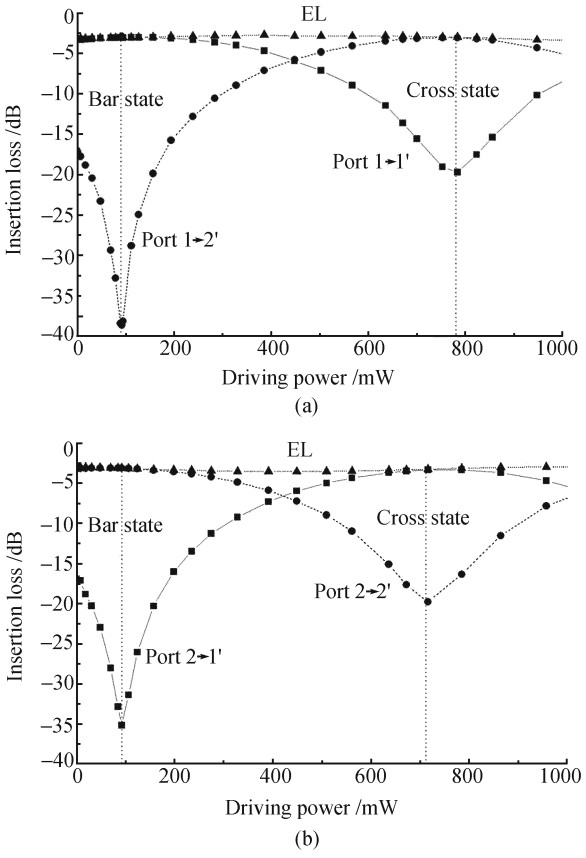

Fig. 3 Relation between IL and driving power
(a) Input from port 1; (b) Input from port 2: EL-excess loss

Table 1 Specifications of the 2 × 2 optical switch

	Input from port 1	Bar	Cross		Input from port 2	Bar	Cross
	Power/mW	92	784		Power /mW	92	716
	IL/dB	3.06	–	2→1′	IL/dB	–	3.40
1→1′	PDL/dB	0.37	–		PDL/dB	–	0.47
	Crosstalk/dB	–	– 19.73		Crosstalk/dB	– 35.18	–
	IL/dB	–	3.10		IL/dB	3.17	–
1→2′	PDL/dB	–	0.23	2→2′	PDL/dB	0.33	–
	Crosstalk/dB	– 38.65	–		Crosstalk/dB	–	– 19.82
	ER/dB	35.59	16.63		ER/dB	32.01	16.42

Note: IL—insertion loss; PDL—polarization dependent loss; ER—extinction ratio, difference between IL and crosstalk

According to the switch principle, original phase difference of the MZI arms is zero and the switch connection is in cross state. While in testing, we need a bias voltage (corresponding to the first bottom of the curves) to reach bar state. The reason is that, adding electrode on waveguide changes effective index of the waveguides. Detailed analysis will be shown in Sect. 4. Switching voltage (corresponding to the second bottom of the curves) shows a slight difference when the input from port 1 or port 2. This results from process error. The difference between driving power corresponding to bias voltage and switching voltage is 658 mW. When bias voltage is reduced to zero after optimization design, this is the switching power. Excess loss (EL, sum of two outputs relative to the input) varies a little from 3 dB when the driving power changes, IL is 3.40 dB. Crosstalk corresponding to bar state and cross state is −35.18 dB and −19.73 dB respectively. The ER is 32.01 dB and 16.42 dB. ER at bar state and cross state is asymmetric. Detailed analysis will be shown in Sect. 4.

3.3 Bandwidth test

Characteristics of the switch within 1 530–1 570 nm wavelength range was measured with EXFO IQS12004B DWDM optical passive devices test system. Driving power was set as the bottom positions of Fig. 3 curves and the test results are shown in Fig. 4. Here we only present the results when input from port 1. Fig. 4(a) corresponds to the lower driving power for bar state and Fig. 4(b) corresponds to the higher driving power for the cross state. The maximum PDL within the wavelength range was measured simultaneously and is listed in Table 1.

We can find that IL and the crosstalk vary a little within the wavelength range and show good bandwidth characteristics. PDL varies much and the maximum PDL within wavelength range is 0.47 dB. Figure 4 shows that crosstalk at bar state is about −30 dB, which is worse than test results in Fig. 3 for a single wavelength of 1.55 μm. This is due to polarization dependence of crosstalk. Figure 4 also shows that crosstalk at bar state is much better than that at cross state.

Test results for a single 2 × 2 MMI coupler are shown in Fig. 5. Splitting ratio is closer to 50 : 50 when the wavelength shifts toward the longer end. Splitting ratio is complementary when input to different ports and was measured as 53.14%

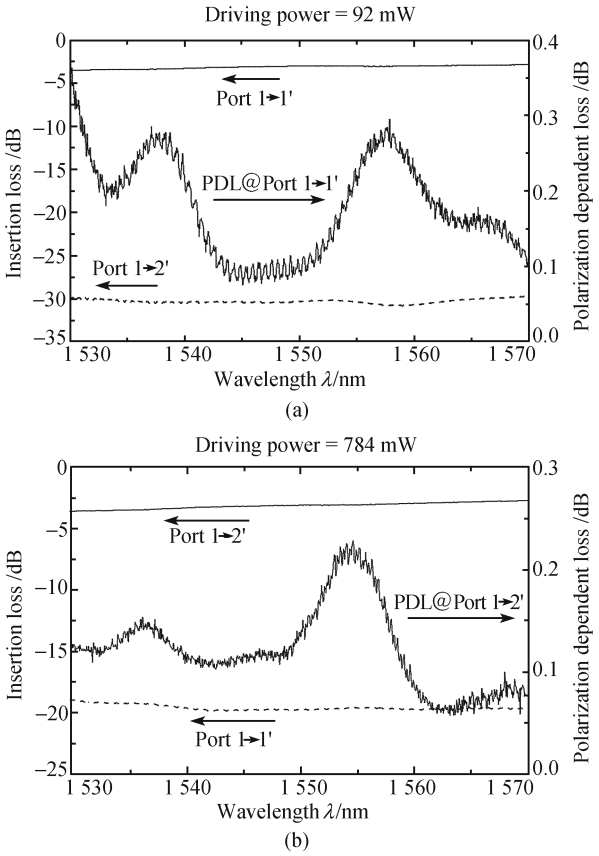

Fig. 4 IL, PDL and Crosstalk properties in 1 530–1 570 nm wavelength span
(a) Lower driving power, bar state; (b) Higher driving power, cross state

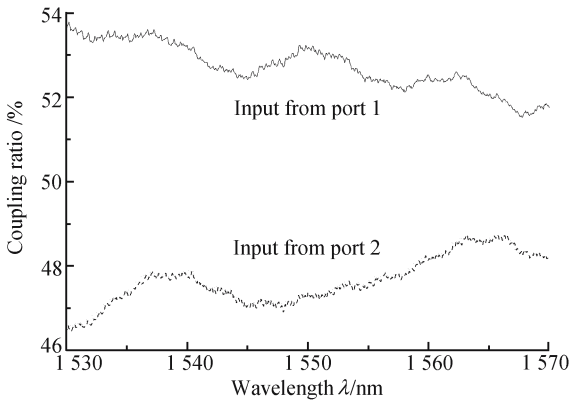

Fig. 5 Bandwidth properties of 2 × 2MMI

and 47.32% at 1.55 μm, which deviates from the destination by 3.14% and –2.68% respectively. At 1.55 μm, EL was measured as 1.81 dB and 1.67 dB respectively with input to different ports, including coupling loss with FAs.

3.4 Response test

The test equipments include Agilent 33120A signal generator, Tektronix TDS3014B oscilloscope, a tunable laser module in EXFO IQS12004B DWDM optical passive devices test system and Advantest Q8221 multi-channel power meter. Response characteristics were tested as shown in Fig. 6. The response time is less than 3 ms, defined as the delay from one stable state to another stable state, while not 10%–90% rising time or dropping time for digital signal process.

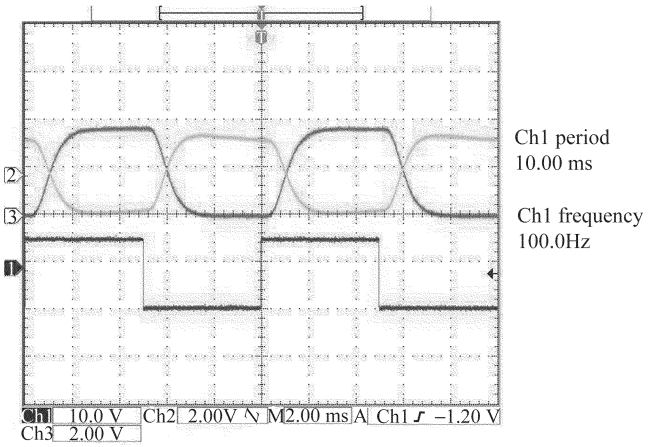

Fig. 6 Response property of the optical switch

4 Results analysis

4.1 Asymmetric splitting ratio for bar state and cross state

Considering splitting ratio error δ resulting from the process error, splitting ratio of 2×2 MMI is $(0.5+\delta) : (0.5-\delta)$ and its transfer matrix is shown as Eq. (3). Correspondingly, transfer matrix of the switch is modified as Eq. (4).

$$\boldsymbol{T}_{\mathrm{MMI}} = \begin{vmatrix} \sqrt{0.5+\delta} & \mathrm{j}\sqrt{0.5-\delta} \\ \mathrm{j}\sqrt{0.5-\delta} & \sqrt{0.5+\delta} \end{vmatrix} \tag{3}$$

$$\boldsymbol{T}_{\mathrm{SW}} = \begin{vmatrix} 2\delta\cos\dfrac{\phi}{2} - \mathrm{j}\sin\dfrac{\phi}{2} & \mathrm{j}\sqrt{1-4\delta^2}\cos\dfrac{\phi}{2} \\ \mathrm{j}\sqrt{1-4\delta^2}\cos\dfrac{\phi}{2} & 2\delta\cos\dfrac{\phi}{2} + \mathrm{j}\sin\dfrac{\phi}{2} \end{vmatrix} \tag{4}$$

Considering good uniformity of the PLC process, two MMI couplers in one wafer are nearly the same. In Eq. (4), two MMI couplers take the same splitting ratio, i.e. their splitting ratio errors are the same. Derived from Eq. (4), crosstalk for bar state and cross state is as follows

$$\begin{cases} \mathrm{Crosstalk}_{\mathrm{bar}} = \cos^2\dfrac{\phi(\lambda)}{2} \\ \mathrm{Crosstalk}_{\mathrm{cross}} = \sin^2\dfrac{\phi(\lambda)}{2} + 4\delta^2 \end{cases} \tag{5}$$

Besides crosstalk resulting from wavelength dependency of MZI arms, compared with bar state, there is one more item $4\delta^2$ for cross state. This item results from splitting ratio error

of MMIs. ER is the difference between crosstalk and IL, so it also shows asymmetry. Crosstalk is less than –30 dB when $\delta < 1.5\%$.

4.2 Original state of optical switch

As shown in Fig. 3, switch connection is not at the desired cross state when driving power is zero. The measured splitting ratio is $95.9\% : 4.1\%$ and $4\% : 96\%$ respectively with input to port 1 and port 2. This is because electrode on waveguide changes its effective index and thus original phase difference of MZI arms is not zero. Phase difference can be described as follows

$$\phi = \phi_e + \phi_t \tag{6}$$

where $\phi_e = 2\pi\Delta n_e L_e / \lambda$ is phase difference induced by electrode. Δn_e is effective index increment due to electrode and L_e is electrode length. $\phi_t = 2\pi\Delta n_t L_e / \lambda$ is phase difference induced by heating electrode. Δn_t is effective index increment due to heating.

Original state measured as Fig. 3 is for central wavelength and thus our analysis takes $\lambda = \lambda_0$, $\phi_t = 0$ for original state and thus $\phi = \phi_e$. According to Eq. (4), the original splitting ratio is $\sin^2(\phi_e / 2) : \cos^2(\phi_e / 2)$ or vice versa with input to port 1 or port 2. Compared with the measured original splitting ratio (take the mean value $95.95\% : 4.05\%$), we get

$$\sin^2 \frac{\phi_c}{2} : \cos^2 \frac{\phi_c}{2} = 95.95\% : 4.05\% \tag{7}$$

According to Eq. (7), phase difference induced by electrode is $\phi_e = 0.871\pi$ and thus $\Delta n_e \approx 2 \times 10^{-4}$. This is effective index increment induced by the electrode on the waveguide. This value doesn't mean general but varies with electrode material and thickness. Adding electrode on both MZI arms can eliminate the influence.

5 Conclusions

Experimental results of a MZI type 2×2 integrated thermooptic switch based on MMI couplers are presented. The IL is 3.40 dB, PDL is 0.47 dB, ER for bar state and cross state is 32.01 dB and 16.42 dB respectively, response time is less than 3 ms and power consumption is 658 mW. After parameter optimization and process improvement, reducing upper cladding thickness and adding isolation slot at both sides of the MZI arms, IL, PDL, ER, response time and power consumption can be improved as 2.20 dB, 0.20 dB, 30 dB, 1 ms and 200 mW, respectively. Theoretical analysis is first presented for asymmetric ER at bar state and cross state. The influence of electrode on effective index of waveguide is analyzed. Further research will focus on optimization of 2×2 MMI couplers to improve its splitting ratio uniformity and bandwidth characteristics, thermal analysis of the switch to reduce power consumption and response time and other detailed process to reduce IL and PDL.

References

1. Yu Peidong, Wang Guozhong, Chen Minghua, et al. Recent progress in optical switching. Semiconductor Optoelectronics. 2001, 22(3): 149–154 (in Chinese)
2. Luo Yuan, Fu Hongqiao, Huang Shanglian. Study on a MEMS silicon-based non-silicon mirror for an optical switch. Chinese Optics Letters, 2003, 1(10): 616–618
3. Lai Q, Hunziker W, Melchior H. Low power compact 2×2 thermooptic silica-on-silicon waveguide switch with fast response. IEEE Photon. Technol. Lett., 1998, 10(5): 681–683
4. Yu Jinzhong, Chen Shaowu, Xia Jinsong, et al. Progress in SOI based optical waveguide devices and integrated optical switch matrix. Science in China Ser. E, 2004, 34(10): 1081–1093 (in Chinese)
5. Wang Fan, Yang Jianyi, Chen Limei, et al. Optical switch based on multimode interference coupler. IEEE Photon. Technol. Lett., 2006, 18(2): 421–423
6. Wei Yuan, Seongku K, Willim H S, et al. Electrooptic polymeric digital optical switches (DOSs) with adiabatic couplers. IEEE Photon. Technol. Lett., 2005, 17(12): 2568–2570
7. Yang Jianyi, Jiang Xiaoqing, Yang Fanghui, et al. 2×2 Total-internal-reflection optical switch using thermo-optic effect of polymer. Chinese Journal of Lasers, 2003, 30(2): 137–140 (in Chinese)
8. Yang Jianyi, Jiang Xiaoqing, Yang Fang hui, et al. Polymer optical switch with Y-branch. Acta Optica, Sinica, 2002, 22(6): 735–738 (in Chinese)
9. Huang Xutao, Jiang Xiaoqing, Yin Rui, et al. Characteristics of GaAs heterostructure BOA type optical switches. Acta Photonica Sinica, 2001, 30(2): 157–161 (in Chinese)
10. Bachmann M, Besse P A, Melchior H. General self-imaging properties in $N \times N$ multimode interference couplers including phase relations. Appl. Opt., 1994, 33(18): 3905–3911
11. Lucas B S, Erik C M P. Optical multi-mode interference devices based on self-imaging: principles and applications. J Lightwave Technol, 1995, 13(4): 615–627